Structural and optical characterisation of holey fibres using scanning probe microscopy

C.W.J Hillman, W.S. Brocklesby, T.M Monro, W. Belardi and D.J Richardson

We present what we believe is the first investigation of a holey fibre using scanning probe microscopy techniques. Atomic force microscopy (AFM) images provide knowledge of the fibre structure without the artefacts associated with SEM imaging. A tapered fibre SNOM probe has been used to investigate holey fibre modes at 785nm.

Introduction: A holey fibre (HF) is an optical fibre with optical properties and confinement mechanism defined by air holes that run the entire length of fibre, an example is shown in Fig.1. These holes define the cladding region of the fibre. Light is guided in the solid core due to effective refractive index contrast between core and cladding [1]. This index contrast can be considerably larger than in conventional fibre, leading to the potential for highly confined modes with small mode areas and high effective nonlinearity. The effective cladding index is also strongly wavelength dependant, which leads to a range of novel optical properties such as endlessly single moded guidance [1] and anomalous dispersion below 1.3μm [2,3].

Current structural characterisation of HF relies upon light and scanning electron microscopy (SEM) techniques. However, these techniques

have practical considerations that limit their usefulness in imaging HF. Light microscope resolution limits mean that this approach cannot yield precise information regarding absolute or even relative feature sizes. Since fibre properties such as dispersion and birefringence can be sensitive to the precise details of the hole arrangement, especially when the core dimensions are small, this knowledge is crucial to the development of HF. SEM provides a solution to this problem in large scale HF when the features are relatively large (>1μm). However when an SEM image is made it is generally necessary to evaporate a conducting metal film onto the fibre; this film can significantly distort any small-scale features, making it difficult to obtain an accurate measure of the cladding configuration.

Current techniques for characterising HF modes rely on the use of standard relay optics and imaging equipment. The tight mode confinement possible in fibres like the one shown in Fig.1 presents challenges in terms of spatial resolution and dynamic range, and the high NA in such fibres compounds this problem. Here we present solutions to these structural and modal profiling problems with the application of scanning probe microscopy (SPM) techniques.

The microstructured part of the HF used in this investigation was fabricated by stacking silica capillaries around a solid core rod. The microstructured region is jacketed and pulled down to fibre with an outer diameter of 125μm. An SEM image of this fibre is shown in Fig 1. The resulting fibre is robust, can be produced in long lengths, and has a microstructured region ~9.5μm in diameter and a core diameter of ~1.25μm.

Results: In order to more accurately establish the real structure of the fibre and to investigate the effect of the gold coating used in the SEM, a cleaved fibre end was scanned with an AFM. A Burleigh Vista AFM was used in contact mode with a tetrahedral tip with an apex half angle of ~25°. The image obtained (Fig. 2) clearly shows both the capillary voids and the interstitial holes caused by the packing of the capillaries.

The inset to Fig. 2 shows cross-sections of the topography data along the two optical axis of the fibre including the four most optically significant holes. The effect of the convolution of the tip shape with the surface profile can clearly be seen. This convolution is unimportant for our application since only the location and dimensions of the features are interesting, rather than the detail of the feature edges themselves. By using the break point of the topography curve as the tip scans over the edge, it is possible to make accurate measurements of the edge location. In the image shown the limiting factor on resolution is the pixel size since a large area was being scanned. Scanning a smaller area, the resolution is increased correspondingly. The limit on the resolution is the AFM tip radius and which is typically of order 10nm. Using this topograph accurate fibre cross-sectional profiles can be measured. By comparison of the SEM and AFM topography an estimate of the discrepancy between SEM and actual fibre dimensions can be made. The SEM image data needs to be arbitrarily thresholded in order to derive a cross-sectional profile, and the net uncertainty introduced by the combination of this process and the uncertainty in the thickness of the gold coating at the fibre edge can be estimated to be ~100nm

The accurate AFM topography has been used to predict the modes of propagation supported by the fibre using the hybrid orthogonal function method described in Ref. 3. This approach can directly model real fibre profiles, and an accurate fibre cross-sectional profile is necessary to give a good description. Fig 3 shows the refractive index profile obtained from the AFM data superimposed with the theoretically predicted mode at 785nm (dashed contours). It is possible to see the strong confinement caused by the ring of four small holes around the core. The predicted mode shown has a $1/e^2$ radius in the horizontal axis of 0.632 μm.

To obtain a direct experimental measurement of the near field mode profile, we have applied technologies developed originally for scanning near field optical microscopy (SNOM). The SNOM probe samples the Poynting vector of the optical field at a given point [4]. By using a tip dithering mechanism, and monitoring the amplitude of oscillation it is possible to lock the probe to within ~10nm of the sample using a shear force feedback technique [5].

The tip used in this experiment was fabricated using a Sutter P-2000 pipette puller to taper a single mode optical fibre to a diameter of ~100nm. This tip was then coated by the oblique evaporation of aluminium in order to prevent light from entering the tip other than via the small aperture at its end. The non-tapered end of the tip fibre is incident on a photomultiplier tube that enables the counting of single photons. This gives a large dynamic range (>40dB) that is difficult to obtain with other imaging techniques. The HF is mounted on a 3-axis piezoelectric actuated stage to allow accurate height regulation and the scanning of the mode profile via computer control. Scans

were taken in two modes: contact mode, in which the tip is held ~10nm from the surface by shear force feedback and follows the surface topography, falling down the holes that are present in the sample, or constant height mode. This latter mode enables any artefacts due to tip z-motion to be removed, but means that the tip has to be held further from the surface (>100nm). The non-contact mode scans are not shown for brevity.

The greyscale image in Fig.3 shows the data collected in a SNOM scan. Topographical information can also be extracted from the SNOM scan, though because of the larger tip and step size, the small holes cannot be resolved as well as in the AFM image. The inset to Fig. 3 shows a cross-section from both the SNOM data and theoretical predictions where a good agreement can be seen. The small discrepancy between the modes can be attributed to two main factors. Firstly, the field is not sampled at a single point but within a finite area defined by the ~100nm diameter probe tip which leads to a slight broadening of the observed profile. For these measurements the experimental $1/e^2$ width was 0.710μm, as opposed to our theoretical estimate of 0.632μm. The difference in these estimates is consistent with the broadening error expected for a 100nm diameter probe. It is to be appreciated that the mode size in this fibre is extremely small, indeed we believe it to be the smallest value yet measured for a holey fiber. The second source of differences between the modelled and measured mode profiles is the presence of low intensity guided cladding modes excited by leakage from the central mode, these cladding modes have not been included in the theoretical model.

Conclusion: In conclusion, we report the application of AFM and SNOM to determine both structural and modal holey fiber properties. We

consider that such scanning probe microscopes will ultimately prove invaluable tools with which to better characterise the unique and exciting properties of this rapidly emerging new class of optical fibre.

References

1 T.A.Birks, J.C.Knight, and P.St.J.Russell, "Endlessly single-mode photonic crystal fiber," Optics Letters, 1997, **22**, 961-963

2 D.Mogilevtsev, T.A.Birks, and P.St.J.Russell, "Group-velocity dispersion in photonic crystal fibers", Optics Letters. 1998, **23**, 1662-1664

3 T.M.Monro, D.J.Richardson, N.G.R.Broderick, and P.J.Bennett, "Holey optical fibers: an efficient modal model," IEEE Journal of Lightwave Technology, 1999, **17**, 1093-1102

4 D. Courjon and C.Bainier, "Near field microscopy and near field optics", Reports on Progress in Physics. 1994, **57**, 989-1028

5 K. Karrai and R. D. Grober, "Piezoelectric Tip-Sample Distance Control for near-Field Optical Microscopes", Applied Physics Letters, 1995, 66 (14), 1842-1844.

Author's Affiliations:

C.W.J. Hillman, W.S. Brocklesby, T.M Monro, W. Belardi and D.J. Richardson (Optoelectronics Research Centre, University of Southampton. Southampton. UK. SO17 1BJ. United Kingdom)

E-Mail:

cwjh@orc.soton.ac.uk

Figure Captions:

Fig. 1. SEM of HF with a 1.25μm core and 125μm outer diameter.
Fig. 2. AFM of the central region of HF in Fig.1. The inset shows cross-sections of this data. All dimensions in μm.
Fig. 3. Contour plot of surface topography, grey scale plot of measured mode profile. Inset shows comparison of theoretical (solid line) and measured mode profiles (points).

Figure 1

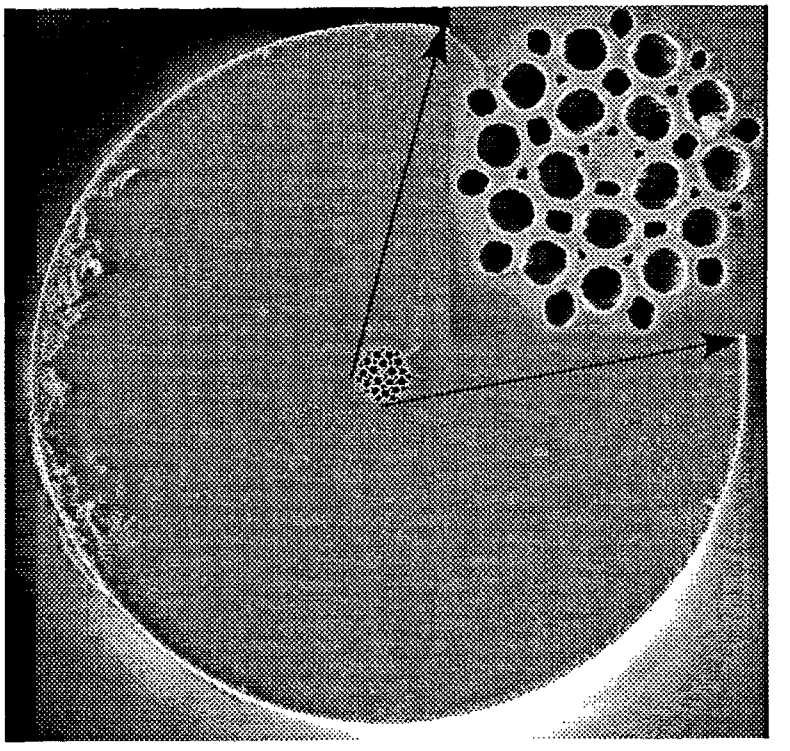

Figure 2

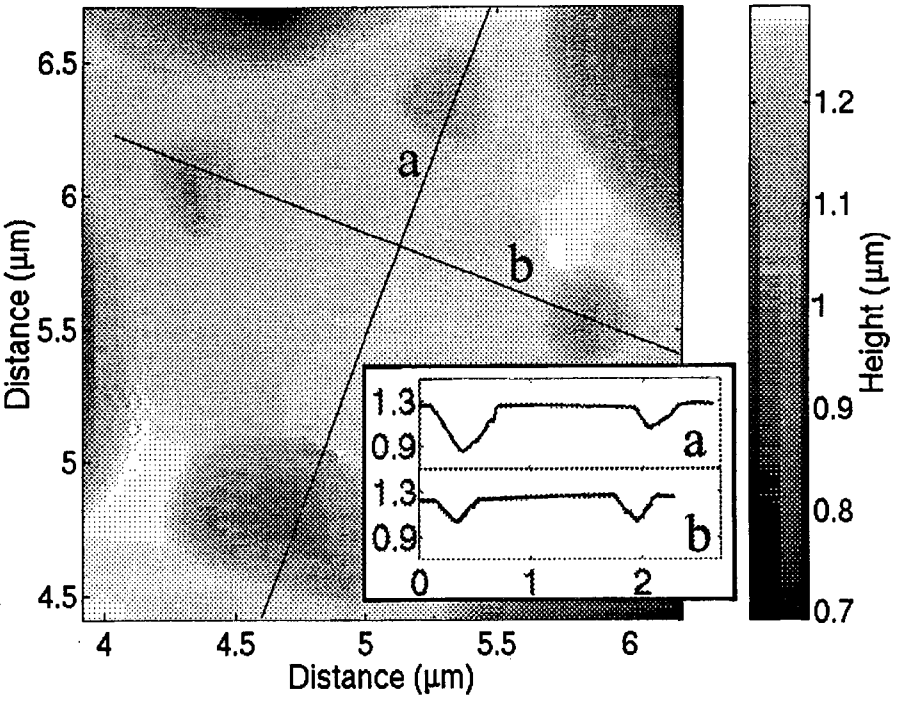
6.5
6
5.5
5
4.5
Distance (µm)
4
4.5
5
5.5
6
Distance (µm)
a
b
1.3
0.9
a
1.3
0.9
b
0
1
2
1.2
1.1
1
0.9
0.8
0.7
Height (µm)

Figure 3

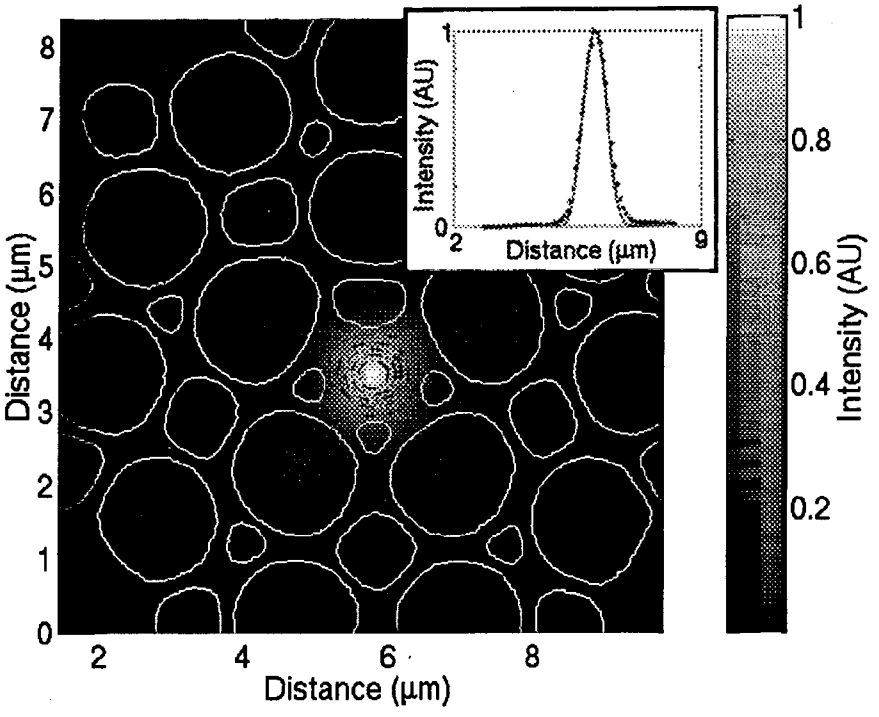
Distance (µm)
Distance (µm)
Intensity (AU)
Intensity (AU)
Distance (µm)
0
1
2
4
6
8
0.2
0.4
0.6
0.8
1
2
9